Pre-proofreading version. Final version can be found in **CMDA 121**(4): 365-384
https://dx.doi.org/10.1007/s10569-015-9604-9

ON THE a AND g FAMILIES OF ORBITS IN THE HILL PROBLEM WITH SOLAR RADIATION PRESSURE AND THEIR APPLICATION TO ASTEROIDS

D. García Yárnoz,[1] D. J. Scheeres[2] and C. R. McInnes[3]

ABSTRACT

The focus of this paper is on the exploration of the a and g-*g'* families of planar symmetric periodic orbits around minor bodies under the effect of solar radiation pressure. An extended Hill problem with solar radiation pressure (SRP) allows the study of spacecraft trajectories in the vicinity of asteroids orbiting the Sun. The evolution of the a and g-*g'* families is presented with SRP increasing from the classical Hill problem to levels characteristic of current and future planned missions to minor bodies, as well as one extreme case with very large SRP for a small asteroid. In addition, the implications of considering a spherical body are analysed, in terms of trajectories colliding with the asteroid and eclipses, which limits the feasibility of various family branches. Finally, the influence of SRP on the linear stability of feasible orbits is calculated.

Keywords: *Asteroids dynamics; Hill problem; Solar Radiation Pressure*

1 Introduction

The influence of a large solar radiation pressure perturbation (SRP) on spacecraft dynamics is of great importance for asteroid exploration missions. For very small bodies SRP is arguably the largest perturbing force for spacecraft with typical effective area and mass. In the course of a previous study (García Yárnoz, Sanchez Cuartielles et al. 2013), the authors encountered and briefly presented a series of periodic solutions propagated with a numerical integrator considering the gravitational attraction of a small asteroid and the Sun, and including SRP and eclipses (see Figure 1). The objective of the study was to propose orbits or other strategies providing complementary coverage to terminator orbits and associated families. That is, trajectories were sought that remain in the vicinity of the asteroid and provide coverage on a plane perpendicular to the terminator, in particular of the sub-solar and anti-solar point regions. The planar periodic solutions in Figure 1, which remain in the orbital plane of the asteroid, are attractive candidates for this purpose and as such they are the focus of this paper and will be analysed in detail. These orbits are symmetric with respect to the x-axis in a synodic frame co-rotating with the asteroid around the Sun (and thus they have two crossings perpendicular to this axis). They have two or more inversions of the orbit direction, that take place when they reach the zero-velocity curves for their particular energy level, alternating between prograde and retrograde sections of the orbit from the point of view of the body. Of particular interest for operations around asteroids would be orbits with retrograde sections close to the asteroid, and prograde ones far from it (e.g. second plot in Figure 1), as retrograde orbits are less affected by the highly non-spherical gravity fields of minor bodies, assuming a prograde rotation of the asteroid, that is, in the same direction as the orbital motion.

[1] Advanced Space Concepts Laboratory, Dept. of Mechanical and Aerospace Engineering, University of Strathclyde, Glasgow G1 1XQ, UK. E-mail: daniel.garcia-yarnoz@strath.ac.uk Telephone: +44 (0)141 444 8316. Fax: +44 (0)141 552 5105

[2] Celestial and Spaceflight Mechanics Laboratory. University of Colorado at Boulder.

[3] Advanced Space Concepts Laboratory. Dept. of Mechanical and Aerospace Engineering, University of Strathclyde

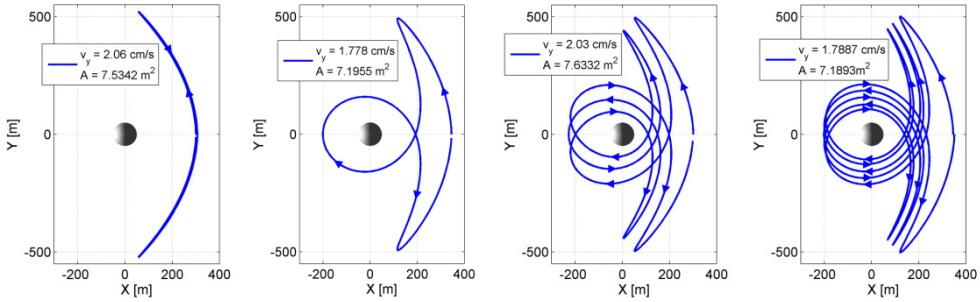

Figure 1: Families of solutions in a co-rotating synodic frame

The first two classes of orbits were identified as members of the a and *g'* families described by Hénon (1969). These families of orbits are a well-known set of solutions of Hill problem, one of the limiting cases of the Circular Restricted Three Body Problem (CR3BP). In particular, the top branch of Hénon's *g'* family greatly resembles the type of orbits with one loop and two inversions that were found in the numerical propagation analysis. The following sections present the evolution of these families when solar radiation pressure is introduced and study the applicability of these orbits for minor bodies. They could represent an alternative to more traditional strategies around very small minor bodies, such as hovering (Broschart and Scheeres 2005; 2007) and pseudo-hovering solutions (Scheeres 2012a), multiple low-velocity flybys (Takahashi and Scheeres 2011), or the well-known terminator orbits (Dankowicz 1993; Scheeres 2007; Byram and Scheeres 2008).

1.1 Families of planar symmetric periodic orbits in the CR3BP and the Hill problem

In his 1969 paper, Hénon explored families of symmetric periodic orbits in the planar case of the CR3BP for a very small secondary (limiting case of Hill). Hénon concentrated on simple-periodic cases (orbits with only two crossings of the x-axis), although the aforementioned branch of the *g'* family has 4 crossings and is thus double-periodic according to Hénon's own definition. N-periodic orbits, or orbits of multiplicity N, are defined as orbits with 2N crossings of the x-axis. With this definition, the type of trajectories presented in Figure 1 are simple-periodic, double periodic, 5-periodic, and 8-periodic (2, 4, 10 and 16 crossings of the x-axis respectively). Hénon systematically mapped the planar problem, studied the in-plane stability, and cross-checked the validity of previous solutions reported by Hill himself, Lord Kelvin, Jackson and the outputs of the more thorough searches by Matukuma (1930; 1932; 1933).

These families have been extensively studied but are still of great interest. Besides the references used by Hénon in his classical series of papers, other authors came across orbits of the a, g and *g'* family, albeit for different mass ratios. Darwin (1897) generated an incomplete map of various classes of orbits for a mass ratio of 1/11 (a fictitious Sun-Jupiter case with a much larger mass for Jupiter), which corresponds to sections of the g-*g'* family. Broucke (1968) presented results for orbit families in the Earth-Moon system. Szebehely and Nacozy (1967) worked on these same sets of periodic obits. Szebehely's book Theory of Orbits (Szebehely 1967) indeed remains to date a classic reference with an extensive study on different families in the CR3BP, mostly for equal masses (the so-called Copenhagen problem), but also reviewing and completing Darwin's and Broucke's work. Hénon also studied, prior to Hill problem, planar symmetric families in the Copenhagen problem as the other limiting case of the CR3BP (Hénon 1965). In fact, the naming convention assigning letters for the orbit families actually spawns from the nomenclature Strömgren introduced for families of solutions for the Copenhagen problem decades before (Strömgren 1922).

Hénon continued studying the vertical stability in the equal masses case (Hénon 1973a) and the Hill problem (Hénon 1973b). Michalodimitrakis (1980) extended this work by studying some 3-dimensional families of orbits branching off from the vertical critical orbits in the planar case. Perko (1982) established the existence of the families a, c, f, g, g', g"… mapped by Hénon (1969) for the case of small mass ratio $\mu>0$. He overlaps his families over Hénon's, showing their similarity. An additional paper of Hénon (2003), in which he came back to the same problem after over 30 years, expanded his search to orbits of higher multiplicity. A few years later, Hénon (2005) revisited once more the Hill problem to study asymmetric periodic solutions.

Finally, Lara and Russell (2006) performed a comprehensive review of the g family for different mass ratios (explaining and comparing, among others, Darwin's (1897) results for the fictitious Sun-Jupiter case or Broucke's (1968) for the Earth-Moon system), and analysed applications of planar and three-dimensional periodic orbits for a Jupiter-Europa mission (Russell 2006; Lara, Russell et al. 2007). Very recently, two papers by Batkhin (2013a; 2013b) presented an algorithm with regularised coordinates to systematically obtain all families of orbits reported by Hénon for the Hill problem and a set of additional families including multiple collisions with the secondary body. Through private conversation with Verrier (2013) to discuss the branching and connections between two-dimensional and three-dimensional families, she reported that she was studying families of period-doubling bifurcations from halo orbits for the Earth-Moon mass ratio (which she denotes U1 and U2), that resemble planar *g'* orbits. She reports a connection with the *g'* family and has proved the existence of this connection also in the Hill problem.

1.2 Extending the Hill problem for the case of a radiating primary

Hill's limiting case of the CR3BP is particularly suited to the study of asteroids, as the mass of the asteroid can be considered negligible with respect to the Sun, leading to very low mass ratios. However, SRP plays an important role around these minor bodies. Its effect on the well-known symmetric periodic orbit solutions of the CR3BP has not been studied in such great detail.

Approaching the often called classical photo-gravitational CR3BP (Chernikov 1970; Simmons, McDonald et al. 1985), Papadakis (1996) studied the evolution of planar symmetric families in the equal masses case (Copenhagen problem) with two radiating bodies. This approximation has interesting applications in the study of accretion disks around binary stars. Markellos et al. (2000) studied the limiting case of Hill for different configurations of the radiating bodies, and later analysed the evolution of families of periodic orbits up to high multiplicity (16-periodic) and their stability (Kanavos, Markellos et al. 2002). A more comprehensive analysis using regularised coordinates and covering symmetric periodic orbits up to multiplicity 81 can be found in Papadakis (2006). These studies limit themselves though to modest solar radiation pressure, applicable to a star-planet case, but falling short for the case of asteroids. Recently, the families of Lyapunov and halo orbits were analysed for a case with modest solar radiation pressure by Katherine and Villac (2010), and Farres and Jorba (2012) concentrated on these families around the L_2 region for the case of a solar sail at asteroid Vesta.

2 The Hill problem with solar radiation pressure

The equations of motion (EOM) of the Hill problem with solar radiation pressure in a synodic rotating frame centred in the secondary take the well-known form:

$$\begin{cases} \ddot{\xi} = 2\dot{\eta} + 3\xi - \xi \Big/ \left(\xi^2 + \eta^2 + \zeta^2\right)^{3/2} + \beta \\ \ddot{\eta} = -2\dot{\xi} - \eta \Big/ \left(\xi^2 + \eta^2 + \zeta^2\right)^{3/2} \\ \ddot{\zeta} = -\zeta - \zeta \Big/ \left(\xi^2 + \eta^2 + \zeta^2\right)^{3/2} \end{cases} \tag{1}$$

where distances are normalized by d and scaled by $\mu^{1/3}$, and time is normalized by $1/\Omega$, with the mass parameter ratio μ, and mean motion Ω given by:

$$\begin{aligned} \mu &= \mu_{\mathrm{A}} / (\mu_{\mathrm{A}} + \mu_{\mathrm{S}}) \\ \Omega &= \sqrt{(\mu_{\mathrm{A}} + \mu_{\mathrm{S}}) / \mathrm{d}^3} \end{aligned} \tag{2}$$

The Sun or more massive radiating body is assumed on the left (contrary to the convention used in Szebehely 1967), d is the radius of the circular orbit of the asteroid around the Sun, and μ_{A} and μ_{S} are the gravitational constants of the asteroid and the Sun, respectively. These are equivalent to the EOM defined in Byram and Scheeres (2008) or Broschart et al. (2013). The so-called lightness number β (McInnes 1999) in Eq. (1) represents the ratio of the solar radiation pressure and the gravitation of the Sun, scaled as well with $\mu^{1/3}$:

$$\beta = \frac{1}{\mu^{1/3}} \frac{\mathrm{LQ}}{4\pi \mathrm{c} \mu_{\mathrm{S}}} \frac{\mathrm{A}}{\mathrm{m}} \tag{3}$$

where L is the solar luminosity, Q the solar radiation pressure coefficient, which depends on the material properties, c is the speed of light, and A/m is the area to mass ratio of the spacecraft. The solar radiation pressure force is modelled with the traditional cannon-ball approach, assuming the spacecraft has a constant effective area always perpendicular to the Sun-spacecraft line, with the only component of the force in the radial direction. Eclipses are neglected at this stage.

These equations allow an integral of motion Γ, equivalent to Hénon's modified Jacobi constant:

$$\Gamma = 3\xi^2 - \zeta^2 + 2\beta\xi + 2 \Big/ \sqrt{\xi^2 + \eta^2 + \zeta^2} - \dot{\xi}^2 - \dot{\eta}^2 - \dot{\zeta}^2 \tag{4}$$

and are invariant under the following symmetries (Villac 2003; Miele 2010):

$$\begin{aligned} &\Sigma_1 : \left(\zeta, \dot{\zeta}\right) \leftrightarrow \left(-\zeta, -\dot{\zeta}\right) \\ &\Sigma_2 : \left(\mathrm{t}, \eta, \dot{\xi}, \dot{\zeta}\right) \leftrightarrow \left(-\mathrm{t}, -\eta, -\dot{\xi}, -\dot{\zeta}\right) \\ &\Sigma_1\Sigma_2 : \left(\mathrm{t}, \eta, \zeta, \dot{\xi}\right) \leftrightarrow \left(-\mathrm{t}, -\eta, -\zeta, -\dot{\xi}\right) \end{aligned} \tag{5}$$

All symmetries with respect to the η-axis are lost. From the last two symmetries, which comprise a time inversion, if a trajectory satisfies either of the two following conditions at two different times, the resulting orbit will be periodic:

$$\begin{aligned} (\eta, \dot{\xi}, \dot{\zeta}) &= 0 \\ (\eta, \zeta, \dot{\xi}) &= 0 \end{aligned} \tag{6}$$

The first condition translates into finding two perpendicular crossings of the $\xi - \zeta$ plane, and corresponds to three-dimensional periodic families that are out of the scope of this paper, but are presented and studied in Giancotti et al. (2014).

Assuming a planar trajectory ($\zeta = 0$), the second condition implies finding two perpendicular ($\dot{\xi} = 0$) crossings of the ξ-axis. This property is used to find periodic orbits in the extended Hill

problem with SRP. Initial conditions are selected as a perpendicular crossing point of the ξ-axis with positive $\dot{\eta}_0 > 0$. Trajectories are integrated with a Runge-Kutta solver of order 4-5 (Dormand and Prince 1980) and the initial value of $\dot{\eta}_0$ is optimised with a Sequential Quadratic Programming optimisation algorithm (Nocedal and Wright 2006) as implemented in MATLAB's internal functions ode45 and fmincon. The stopping conditions are selected as a second perpendicular ξ-axis crossing, with tolerance in solving the perpendicularity boundary constraint $\dot{\xi} = 0$ of 10^{-9}. In order to avoid orbits with N-multiplicity higher that 2, trajectories with more than one ξ-axis crossing before reaching the stopping condition are discarded.

2.1 The a and g-g' families in the original Hill problem

The former equations of motion reduce to the set studied by Hénon (1969) when equating the lightness number to zero. This set of equations does not depend then on any additional parameter. The same planar periodic families of orbits symmetric with respect to the ξ-axis were reproduced using Hénon's reported values as initial guesses.

The families in the vicinity of the L_2 region are of particular interest due to their possible application to small asteroid exploration. With the introduction of SRP, this region is reduced in size and is closer to the secondary, while the L_1 point migrates far away in the direction of the radiating primary and its associated families of orbits are thus of less interest for close observations of an asteroid. Only simple-periodic families (and a double-periodic branch) were considered as in the original paper by Hénon. Figure 2 represents for reference the traditional Hill problem solution map in the $\Gamma - \xi_0$ space, with ξ_0 representing the initial position along the ξ-axis. The shaded patches represent the forbidden region, given by $\Gamma > 3\xi_0^2 + 2\beta\xi_0 + 2/\xi_0$. An orbit in these regions would require negative kinetic energy.

Figure 3 presents example orbits for the three families analysed: family a (more commonly referred to in literature as planar Lyapunov orbits, top left), originating from L_2; family g (Figure 3 top right, also termed Distant Prograde Orbits or DPOs) evolving from large ribbon-type orbits to circular orbits of decreasing size around the secondary; and subfamily *g'*, emanating from a bifurcation point (black dot marker) and including oval-shaped orbits near the bifurcation (Figure 3 bottom right) and double periodic orbits (with 4 intersections with the horizontal axis, Figure 3 bottom left) after a collision with the secondary (black + marker). This section follows closely the a family in the $\Gamma - \xi_0$ space. Below the bifurcation point the *g'* oval orbits continue extending towards the left until their shape starts deforming with ribbon-like loops again until a second collision point with the secondary at $\xi_0 = 0$. The *g'* family branch shown in the negative ξ_0 quadrant corresponds to the second crossing of the double periodic *g'* orbits.

Families f and c have been included in Figure 2 for completeness. They consist of the sometimes referred to as Distant Retrograde Orbits (DROs) (Ocampo and Rosborough 1993) and planar Lyapunov orbits around L_1 (the symmetric equivalent to family a for L_2). They will not be the focus of this paper thought as their distance to the secondary increases rapidly with lightness number, and thus their usefulness is limited for asteroid observation. A brief description of the evolution and shape of these families with SRP can be found in Appendix A. From this point on, only the positive ξ_0 plane is plotted in the main body of the paper.

Some of the orbits would intersect the secondary if it is not considered a point mass. The asteroid radius (assumed a spherical body) in scaled coordinates, independent of the minor body size, is fixed for a given density ρ and distance between bodies d :

$$\mathrm{R}_{\mathrm{norm}} = \frac{1}{\mathrm{d}} \sqrt[3]{\frac{3\mu_{\mathrm{S}}}{4\pi\rho \mathrm{G}}} \tag{7}$$

where G is the gravitational constant. Family *g'* orbits intersecting the secondary body surface for an average asteroid density of 2.6 g/cm^3 (Chesley, Chodas et al. 2002) and a heliocentric distance of 1 AU are indicated with a dashed blue line in Figure 2. It is not surprising that these regions contain the collision points.

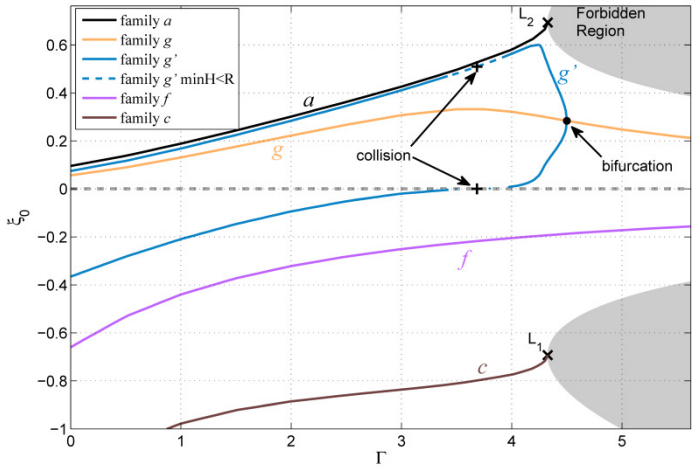

Figure 2: Solution map of the symmetric planar periodic families in the original Hill problem

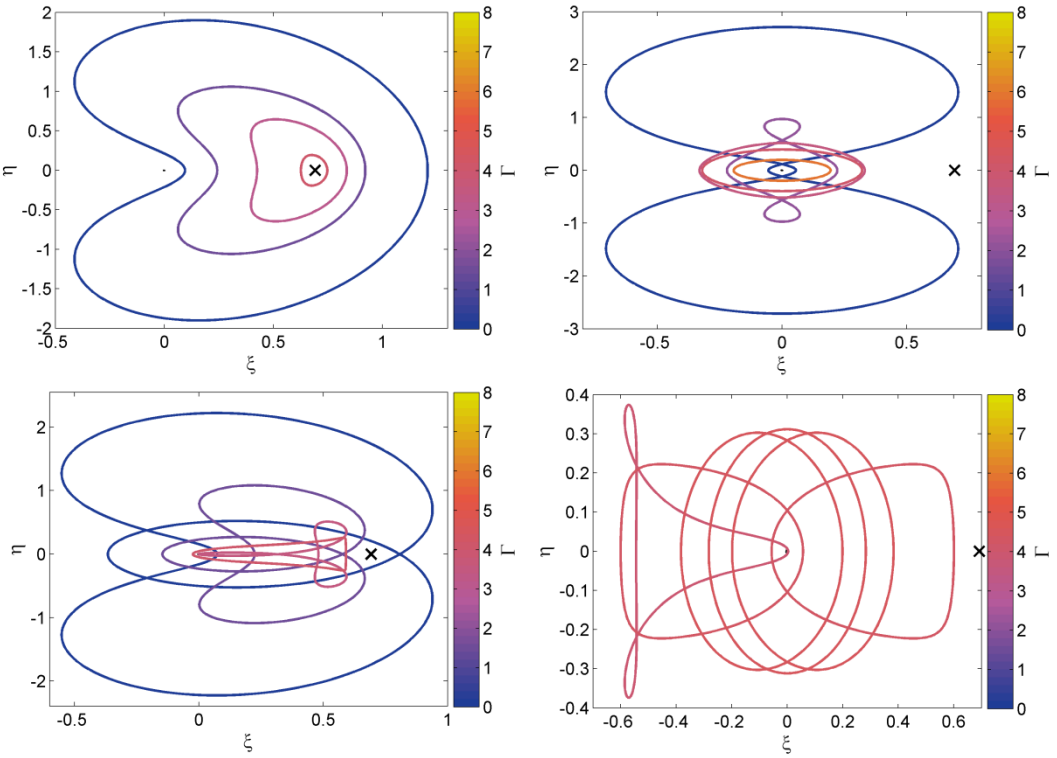

Figure 3: Families a (top left), g (top right) and *g'* (bottom, split in two) in the Hill problem with no SRP. A black x marker indicates the position of the L_2 point.

2.2 Evolution with lightness number

By means of a continuation method, the value of β is increased up to lightness numbers characteristic of asteroid missions. For currently flying and planned minor body orbiters the lightness number is usually of the order of 20-30 (Scheeres 2012c). An extreme case with a β value of approximately 684 is also considered (corresponding to a small 50 m radius asteroid at 1 AU, average asteroid density of 2.6 g/cm^3, 100 kg spacecraft mass and 8 m^2 effective area).

Figure 4 shows the evolution of the families with positive ξ_0 with increasing β. Dashed sections of the families correspond to orbits intersecting the secondary body surface for average NEO asteroid and distance of 1 AU. The horizontal grey dashed line indicates the scaled radius of the secondary. As the lightness number increases, the L_2 point position on the ξ-axis decreases, while its Jacobi constant increases. The bifurcation point of the g-*g'* families disappears immediately for small lightness numbers resulting in two unconnected families (in the plane, there could still be connections through intermediate three-dimensional families). This bifurcation disappears as well in the CR3BP for the case of very small μ, as reported by Perko (1982) and shown for the case of the Jupiter-Europa system by Russell (2006). However, the connection of the branches of the families in the case of small μ is exactly the opposite of the case here presented.

Arbitrarily, the g family was assumed now to contain the branch of the original g family left of the bifurcation point, and the branch of the original *g'* family to the bottom of the bifurcation point (see Figure 4). The *g'* family now contains the top branch of the original *g'*, which includes the collision point and the double-periodic section, and the right branch of the original g family including decreasingly smaller orbits around the secondary. The new g family reduces its size and the maximum ξ crossing decreases rapidly. It then disappears for large lightness numbers. The right branch of the new *g'* family on the other hand quickly tends to skirt the border of the forbidden region, tending to linear degenerate orbits along the ξ-axis. Meanwhile, the collision point that separates the simple and double periodic portions of the new *g'* family migrates towards the L_2 point.

This behaviour is similar to the one observed in the study of radiating equal masses (Papadakis 1996), and continues the results obtained in Kanavos et al. (2002) for small lightness numbers up to 0.33. The following sections show the changes in the shape of the orbits with SRP.

2.2.1 Family a

Figure 5 shows the evolution of the a family from bean-shaped to boomerang-like orbits. To easily display possible intersections with the surface of the secondary, dashed grey circles represent the asteroid surface for densities of 1, 2 and 3 g/cm^3 (circles of decreasing size as the density grows), assuming again a heliocentric distance of 1 AU. They are mostly noticeable for the extreme case with high SRP.

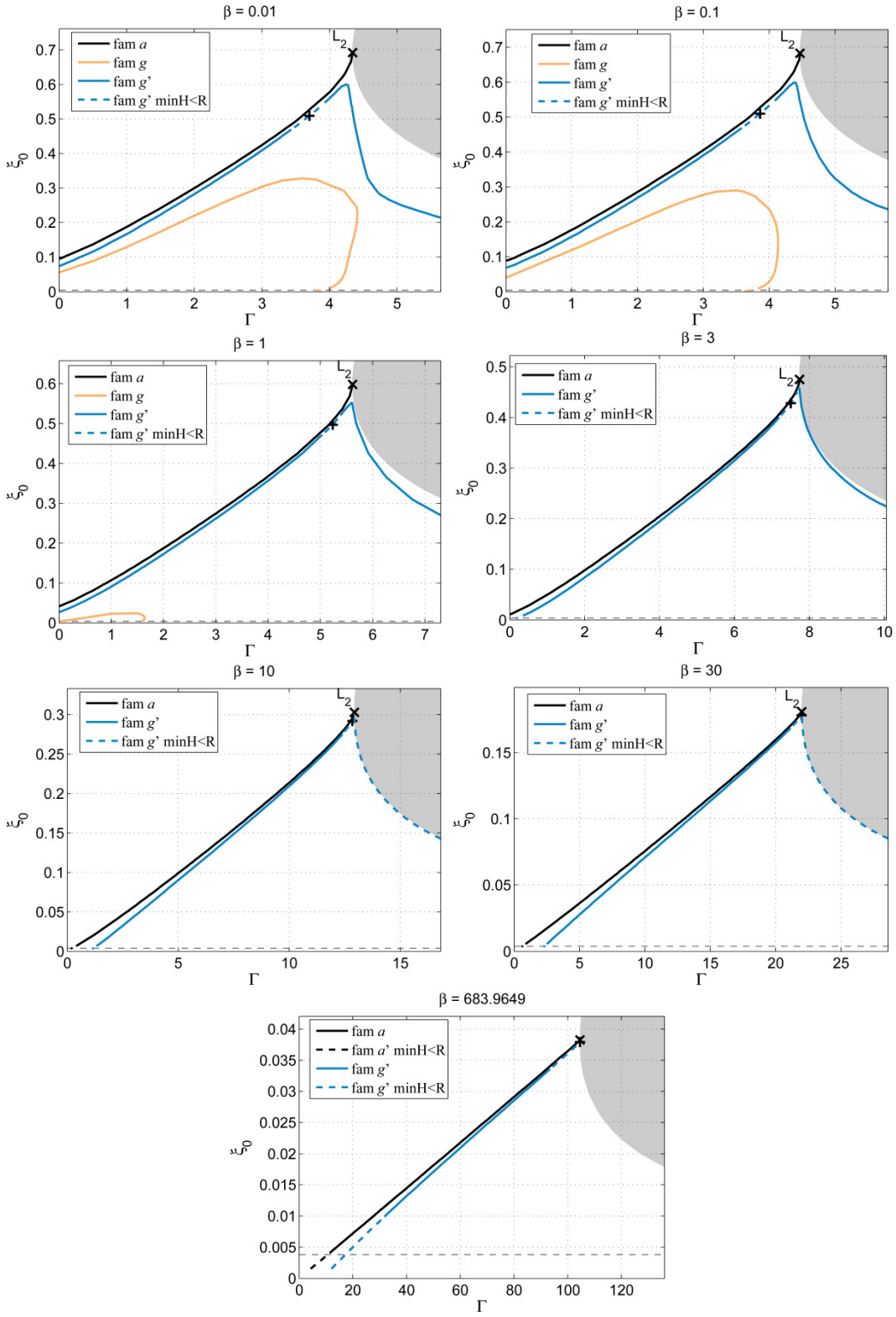

Figure 4: Solution map evolution with increasing lightness number β. The dashed horizontal line shows the radius of the secondary assuming average NEO density and 1 AU distance from the Sun.

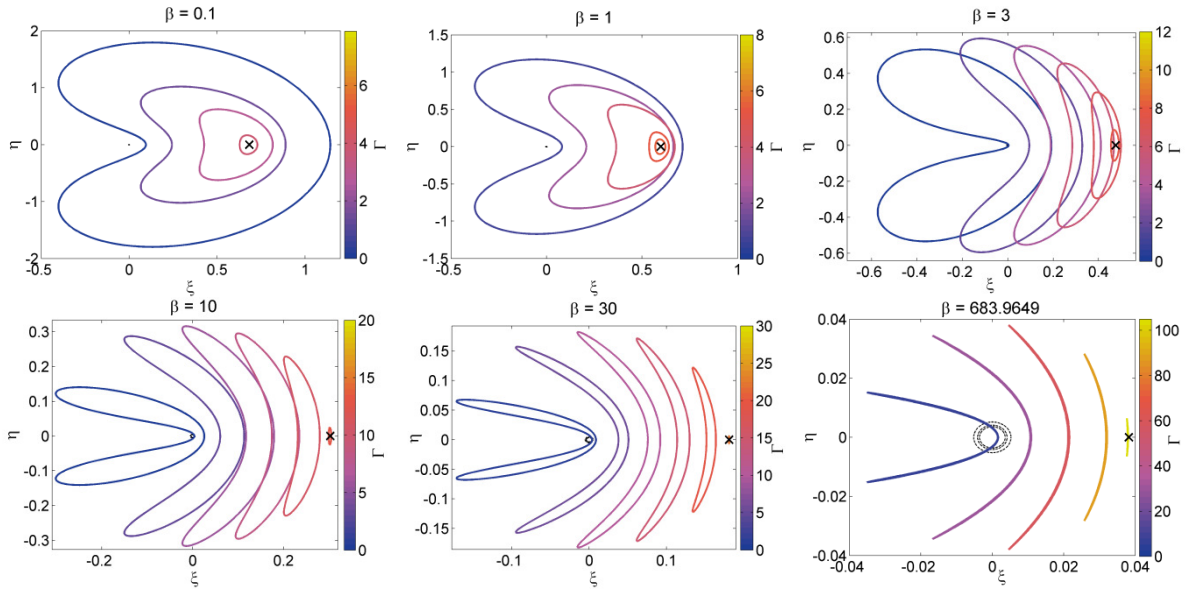

Figure 5: Family a evolution with increasing lightness number. Dashed black circles indicate the asteroid surface for densities of 1, 2 and 3 g/cm^3 and 1 AU distance from the Sun.

2.2.2 Family g-*g'*

Figure 6 plots orbits of the left branch of the *g'* family up to the maximum value of ξ crossing for various Jacobi constants. This includes the double periodic branch left of the collision point along with several oval-shaped simple periodic orbits.

Figure 7 plots orbits of the right branch of the *g'* family from the maximum value of ξ crossing for various Jacobi constants. In the case of no SRP (see Figure 3 bottom right), family *g'* continued with oval-shaped orbits oriented towards the left until the collision point at ξ_0=0. In Figure 7, the branch now includes the former part of the g family which consisted of direct orbits around the secondary of reducing size. With increasing lightness number, this branch tends towards degenerate linear orbits along the ξ axis.

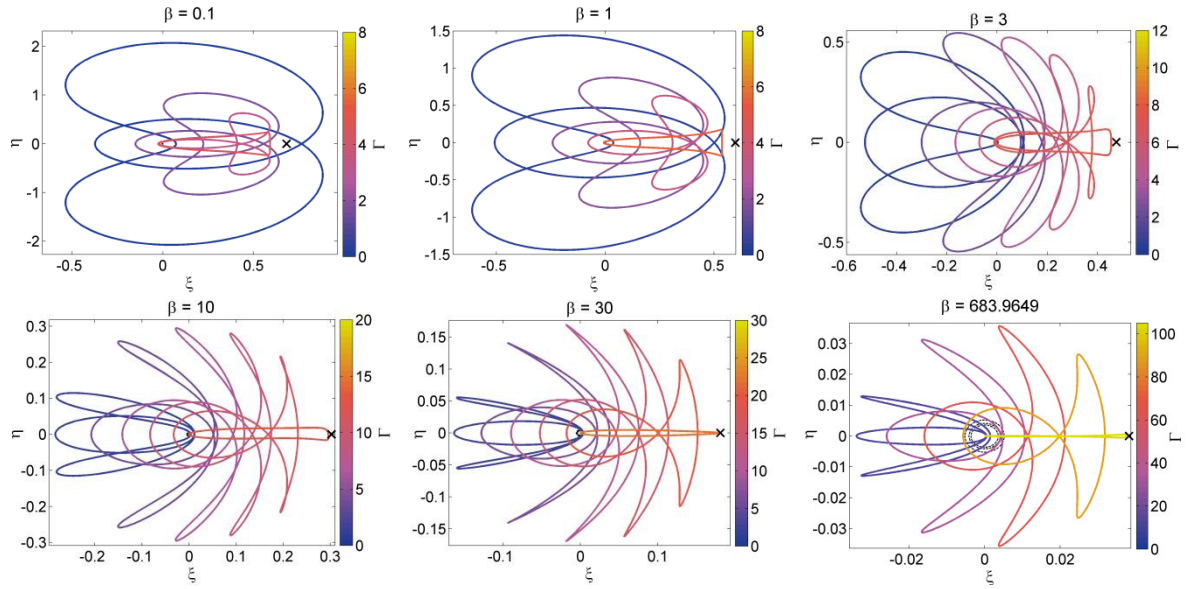

Figure 6: Family *g'* (left branch) evolution with increasing lightness number. Dashed black circles indicate the asteroid surface for densities of 1, 2 and 3 g/cm^3 and 1 AU distance from the Sun.

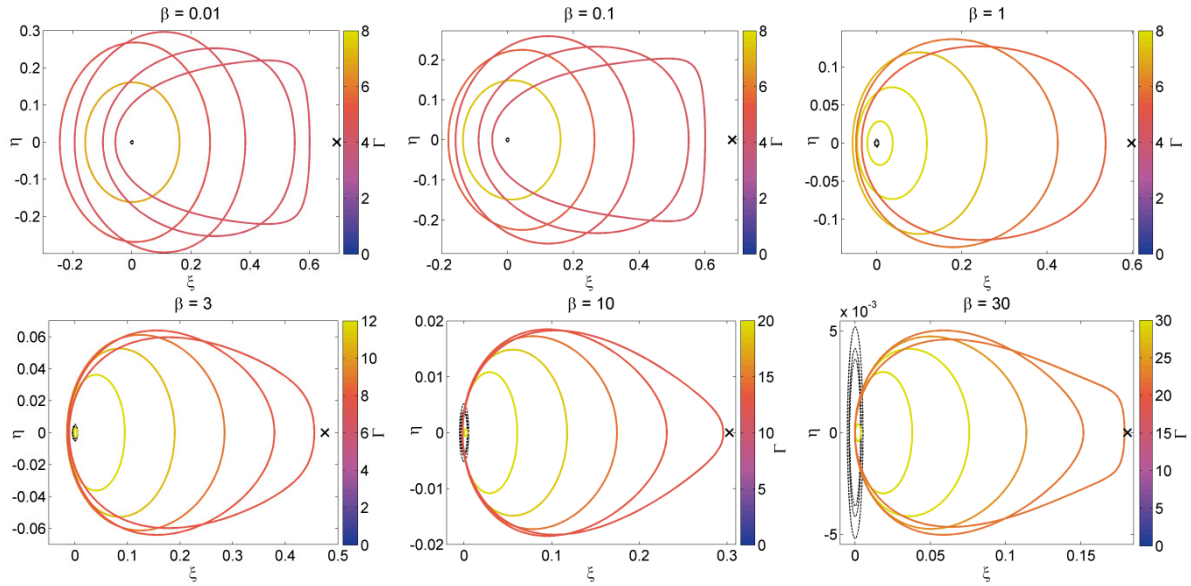

Figure 7: Family *g'* (right branch) evolution with increasing lightness number. Dashed black circles indicate the asteroid surface for densities of 1, 2 and 3 g/cm^3 and 1 AU distance from the Sun.

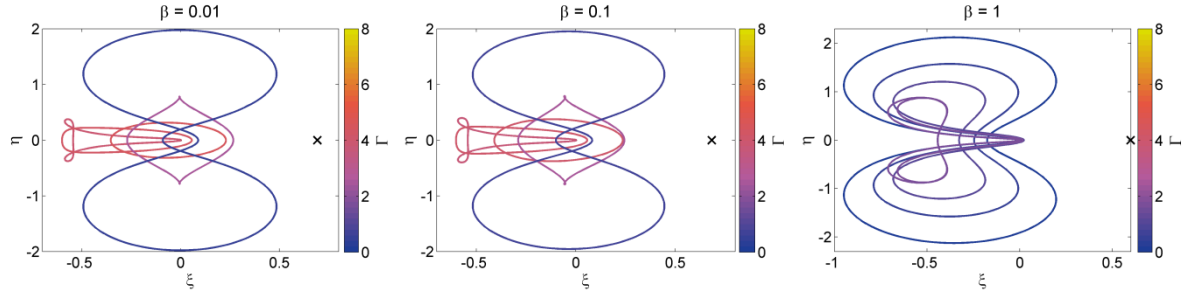

Figure 8: Family g evolution with increasing lightness number

Figure 8 plots orbits of the g family from the maximum value of ξ crossing for various Jacobi constants. Family g now transitions from the ribbon-type orbits in the original g family to the left-extending oval-shape orbits in the original *g'*. For a lightness number of 1 the orbits transition between the two ribbon-type orbits without an oval-shape phase.

3 Application to small asteroids

The above results are an extension of the generic Hill problem with solar radiation pressure, of interest by itself as a dynamical system, and applicable to a variety of problems. When used to model the dynamics of a spacecraft around a small minor body or asteroid, some of the families cease to exist or are significantly modified when the asteroid is not considered as a point mass, due to intersections with the asteroid surface or eclipses. The influence of considering a spherical asteroid is more relevant for higher lightness numbers.

3.1 Feasibility considering intersections with a spherical asteroid

The feasibility of some branches of the reported families is questionable when physical constraints such as the body radius are considered. The right section of the new g' family appears to always intersect the asteroid surface for any realistic density at high lightness numbers (see dashed circles in Figure 7). It is particularly noticeable for the bottom right plot.

In Figure 9 the maximum pericentre height for the right branch of the new *g'* family and the maximum ξ_0 crossing of the g family have been plotted as a function of the lightness number. Horizontal lines indicate radius of the secondary for different densities ranging from 1 to 7 g/cm^3, this last density much larger than the expected values for minor bodies. The distance between the asteroid and the Sun is assumed again to be 1 AU. For lightness numbers higher than 8 the whole right branch of the *g'* family intersects the surface. The lightness number for a few representative asteroid missions are also indicated, showing that only for missions to very large asteroids such as Eros, where low lightness numbers are realistic, is this right branch feasible. The maximum ξ crossing of the g family decreases even more rapidly, falling below the asteroid surface already for values as low as 2. This would render both these family sections unusable for the small bodies that are targeted by future missions such as Hayabusa 2 or OSIRIS-REx.

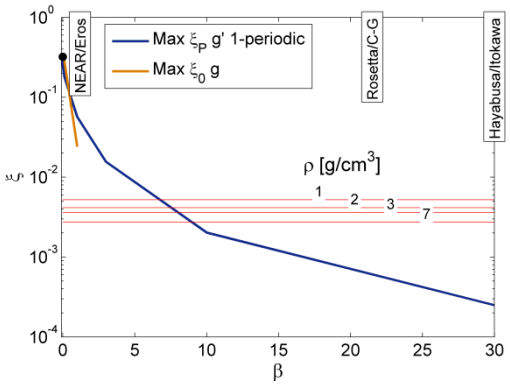

Figure 9: Maximum pericentre height of the simple-periodic *g'* branch and maximum ξ_0 crossing of the g family. For large β they fall below the body surface. Horizontal lines indicate radius of the secondary for different densities ranging from 1 to 7 g/cm^3.

3.2 Effect of eclipses

The consideration of the secondary as a spherical asteroid instead of a point mass has an additional implication on the dynamics due to eclipses. All trajectories of the a and g-*g'* family have portions of the orbit in eclipse, and the eclipses are longer the larger the lightness number (see Figures 6 and 7).

After modifying the solar radiation pressure term assuming a simple cylindrical shadow:

$$\left.\begin{array}{l}\xi > 0 \\ \eta^2 + \zeta^2 \le \mathrm{R}_{\mathrm{norm}}{}^2\end{array}\right\} \Rightarrow \beta = 0 \qquad (8)$$

the a and g' families were recalculated for high lightness numbers. A distance of 1 AU and an average asteroid density of 2.6 g/cm^3 are again assumed to fix the size of the asteroid.

This modification of the SRP term conserves the symmetries in the model, and as such the method to obtain periodic orbits is still valid. However, it introduces a discontinuity in the dynamics, which modifies the solution space. The solution map is plotted in Figure 10 for the cases with high lightness number 30 and ~684. Both families extend beyond the theoretical L_2 point without eclipses, skirting the forbidden region, and the shape of the orbits dramatically changes for the cases spending a considerable time in eclipse (see Figs. 11 and 12).

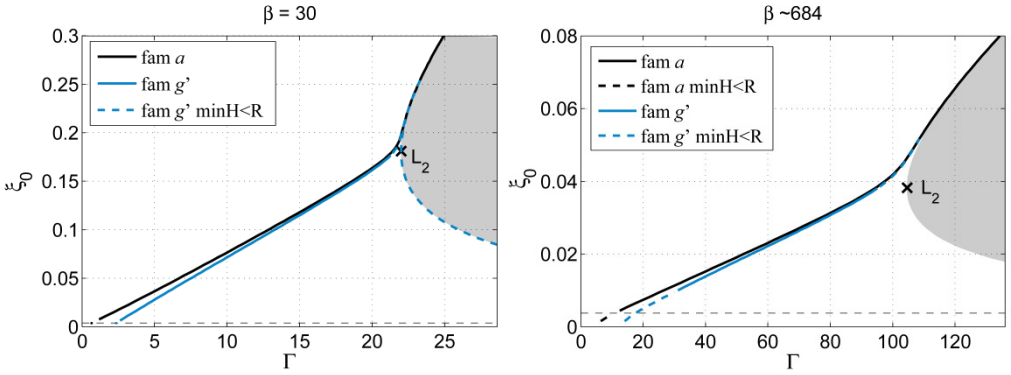

Figure 10: Solution map for the numerical propagation with eclipses. The dashed horizontal line shows the radius of the secondary assuming average NEO density and 1 AU distance from the Sun.

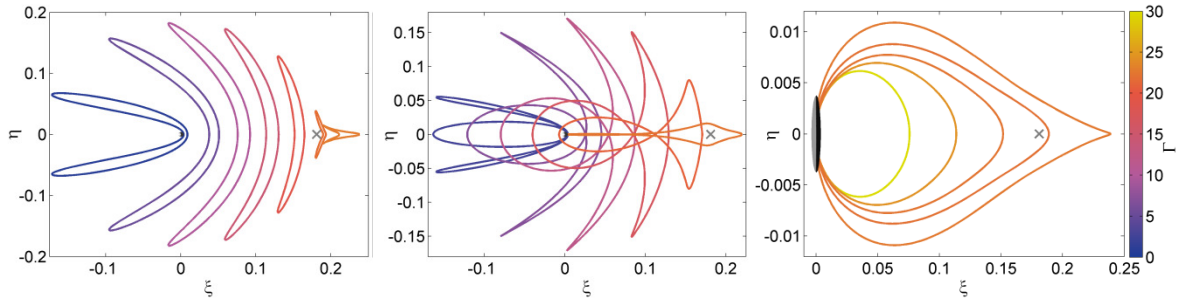

Figure 11: Families a, *g'* left branch and right branch with eclipses. Lightness number $\beta = 30$.

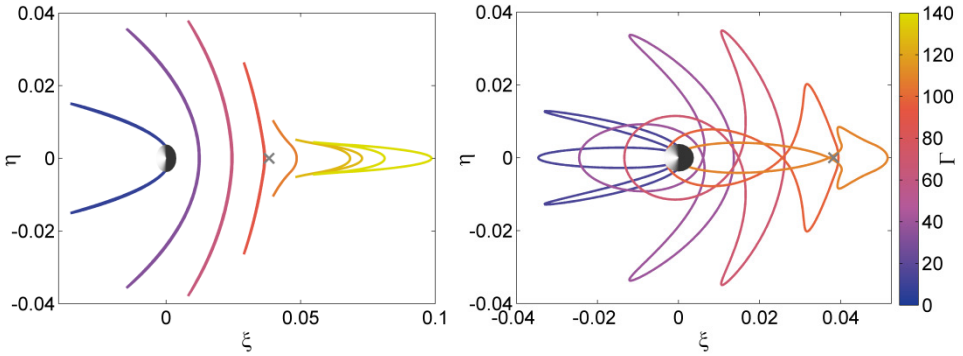

Figure 12: Families a and *g'* left branch with eclipses. Extreme case of $\beta \approx 684$.

4 Stability of *g'* family of periodic orbits

In previous sections, some orbit family branches have been shown to be unfeasible or non-existent for large lightness numbers. On the other hand, for the feasible branches and families, the stability of the periodic orbits needs to be taken into consideration to have usable and practical orbits for asteroid exploration. According to Hénon (1969), in the original Hill problem without SRP all a orbits and all *g'* double periodic are unstable, with two small sections of stable orbits in the simple-periodic branch.

In order to calculate the linear stability using Floquet theory, the state transition matrix is integrated together with the state vector along the trajectory for one orbital period (Scheeres 2012b). The monodromy matrix Φ_M is then obtained by mapping the transition matrix after one revolution to the selected surface of section. The symmetries of the problem and the choice in initial conditions (a perpendicular crossing point of the ξ-axis with positive $\dot{\eta}_0$) implicitly select $\eta = 0$ as a surface of

section. This results in a reduced state vector $\vec{\rho}^* = (\xi, \zeta, \dot{\xi}, \dot{\zeta})$ in which the η and $\dot{\eta}$ coordinates have been eliminated.

For the problem at hand the monodromy matrix results in a sparse 4x4 matrix, where the in-plane and out-of-plane dynamics are decoupled. It can then be split into two 2x2 matrixes and the stability for each type of movement studied separately. The simplified condition for linear stability is then given by $\left|\mathrm{Tr}\left(\Phi_{M,2x2}\right)\right| < 2$ (Scheeres 2012d).

With this stability criteria, family a remains always highly unstable, as was the case when solar radiation pressure was not introduced. The stability index (trace of the 2x2 monodromy matrix) is over two orders of magnitude larger than 2.

Orbits in family *g'* present more interesting properties, with sections of in-plane and out-of-plane stability. Figures 13 and 15 present the stability index for family *g'* as a function of the ξ crossing scaled with the ξ position of point L_2. Orbits are stable for stability index between -2 and 2. For the left branch of family *g'*, including the double-periodic section, orbits are mostly in-plane unstable for low lightness number, but become stable as the lightness number increases towards minor body realistic values close to 30 (see Figure 13 left), with the extreme case of large lightness numbers tending towards stability index equal to 2. Conversely, when considering out-of plane stability (see Figure 13 right), the family displays a somewhat opposite behaviour: the family presents regions of stability for low lightness numbers for certain ranges of ξ-axis crossings. It becomes unstable though as the lightness number increases, and the extreme case tends again to a stability index equal to 2. Figure 14 presents a magnified plot of the out-of-plane stability index close to 2. The crossing points of vertical critical stability represent bifurcations of three-dimensional families that may be of interest.

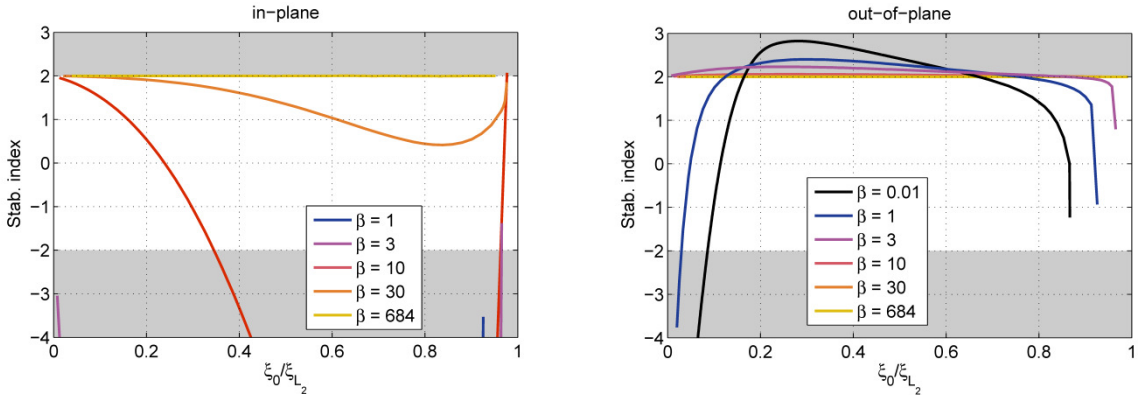

Figure 13: Stability of family *g'* left branch, in-plane (left) and out-of-plane (right)

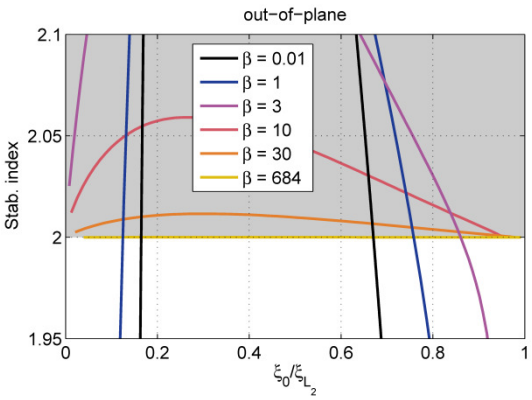

Figure 14: Detail on out-of-plane stability for family g' left branch

On the other hand, the right branch of family *g'*, which is always simple-periodic, seems stable for most of the range when the lightness number is not zero, both in-plane and out-of plane (see Figure 15). That is also the case in the original Hill problem, and it is not surprising as it is comprised of quasi-circular orbits of reduced size around the secondary. Regrettably, these orbits intersect the surface of the secondary for large lightness numbers, questioning their applicability for asteroid exploration. Note also that the behaviour of this branch in the case of no SRP is intrinsically different for low ξ crossings, as it includes a different section of the g-*g'* family.

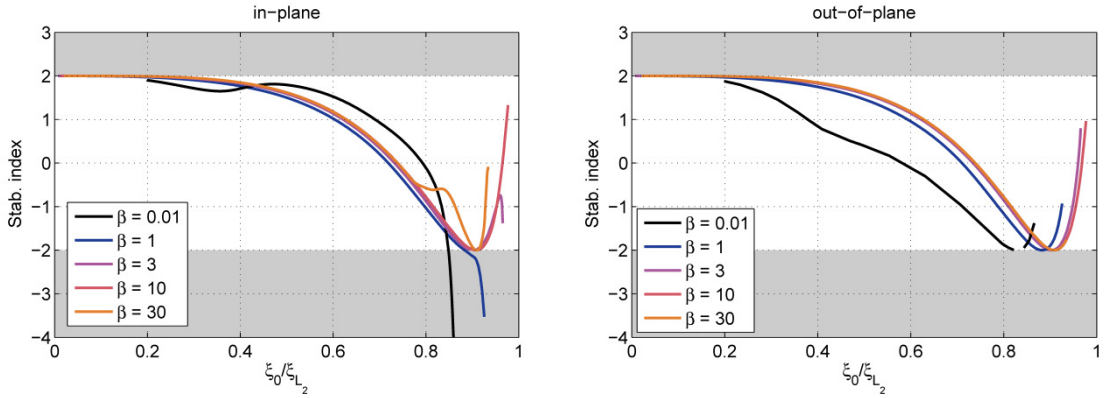

Figure 15: Stability of family *g'* right branch, in-plane (left) and out-of-plane (right)

The region of stability around the g-*g'* family is nonetheless very narrow in the Hill problem, as shown in the Poincaré section in Simó and Stuchi (2000). This behaviour is unfortunately unaffected with the introduction of SRP, and the stable regions are surrounded by a chaotic region which includes escape trajectories.

5 Discussion and model limitations

The analysis presented uses simplified dynamics to study a particular set of planar periodic orbit families in the extended Hill problem with solar radiation pressure. These families of orbits are of particular interest for the exploration of small minor bodies, as the mass ratio is consistent with the Hill approximation and the lightness numbers involved are higher than in usual missions around planets or other larger bodies. They provide alternatives to the current orbit and hovering strategies around asteroids.

The best well-known stable orbits in the vicinity of such small asteroids, i.e., terminator orbits (Dankowicz 1993; Scheeres 2007; Byram and Scheeres 2008), have the drawback of a reduced coverage of the sun-lit side of the asteroid. Associated quasi-terminator orbits (Broschart, Lantoine et al. 2013) have been studied to circumvent this problem. Nevertheless, their coverage of the asteroid close to the sub-solar point is still far from optimal. This limited availability of other stable orbits could make attractive solutions such as the *g'* orbits presented in this paper, which present only a mild instability but cover the asteroid in the XY plane perpendicular to the terminator. Even if regular small corrections would be required to avoid escape or impact, the orbit maintenance costs and frequency of manoeuvres would be significantly reduced when compared to classical hovering or pseudo-hovering strategies such as the one proposed in Scheeres (2012a). Another benefit with respect to hovering is a faster characterisation of the gravity field and mass distribution of the asteroid, as the spacecraft is effectively in orbit. Other strategies such as multiple low-velocity flybys (Takahashi and Scheeres 2011) allow gravity field characterisation but would be slower and less efficient than an orbiting solution. Given the instability of the presented orbits, often resulting in escape solutions after a small number of revolutions, a strategy that combines hold-off points away

from the asteroid with approach to and escape from the *g'* orbits through their associated manifolds would allow for a combination of distant and close-up observations.

The analysis in this paper limits itself to the set of simple-periodic or double-periodic families studied by Hénon (1969). In the course of the study, various exotic and complex orbits were found belonging to higher order periodicity families, still in the planar case (see Figure 16 for a sample of the trajectories found, mostly for low lightness numbers), which have been the subject of a few papers. The higher multiplicity exploration of the Hill problem by Hénon (2003) led to a series of new families, labelled Ha to Hg, some of them stable, albeit without the inclusion of solar radiation pressure. Families up to multiplicity 81 with solar radiation pressure were already reported and studied in literature (Papadakis 2006). The family evolution, feasibility and stability analysis in this paper could be extended to these set of N-periodic families. Despite the beauty of the wide range of solutions, their prospective usefulness is questionable, due to frequent passes close to the asteroid, which could compromise the safety of a spacecraft when additional perturbations are taken into consideration. An additional possible set of families of interest are three-dimensional periodic orbit families bifurcating from the planar ones or from known three-dimensional families such as halo orbits (Katherine and Villac 2010). Other three-dimensional families do exist and can represent alternative orbits for asteroid exploration. The identified vertical critical orbits on the double periodic section of the g' family on Figure 14 are branching points for these additional families. The crossings on the right-hand side of the figure corresponds to the branching of three-dimensional families studied by Verrier (2013), which connect to halo orbits at a double-period bifurcation. When solar radiation pressure increases, this point, together with the collision point, moves rapidly towards the L_2 point. The left-hand side branching point has not been studied in literature to the authors knowledge, but is also rapidly moves towards the collision point at $\xi_0 = 0$.

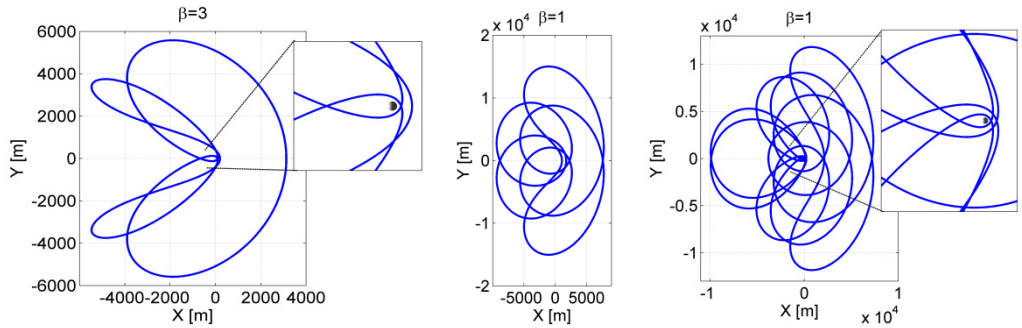

Figure 16: Higher multiplicity family examples: 3-periodic, 5-periodic and 10-periodic.

Perhaps the biggest objection to the applicability of these families to asteroid exploration is that the simple dynamical model used may not effectively represent the range of feasible orbits in a more realistic and complete model. The most obvious extension to this problem is the Elliptic Restricted Three Body Problem (Broucke 1969), or its limiting case the elliptic Hill problem, with the addition of SRP, to account for a more representative case of an asteroid in an elliptical orbit around the Sun. The existence of the a and *g'* family in the elliptic Hill problem has been demonstrated in literature (Ichtiaroglou 1980; 1981). Voyatzis et al. (2012) perform a more detailed analysis of the elliptic Hill problem, extending by continuation to eccentric orbits planar families including stable branches of the higher multiplicity families reported by Hénon (2003). Most orbits are unstable but regions of regular motion can be found around certain families. These orbits could be extended to the case with solar radiation pressure, and their stability properties checked.

However stable the presented symmetric solutions are, this behaviour can quickly change with the introduction of additional perturbations in higher fidelity models. Of particular concern is the non-sphericity perturbation, due to highly irregular shape and mass distribution of asteroids. García Yárnoz et al. (2013) shows that orbits of the double periodic *g'* branch could be found that require limited controllability, for a particular case with a rotating tri-axial ellipsoid. These orbits comprise a retrograde section close to the asteroid, which is least affected by the rotation of the ellipsoid, assuming this rotation is also prograde. A variable area or reflectivity controller is proposed to maintain such an orbit when higher order gravitational harmonics are introduced. Resonant orbits with the asteroid rotation would reduce the required control. Given the uncertainty in the mass, shape and associated gravity field of most asteroids, adjustable area or reflectivity would be a desired feature for orbiters that intend to benefit of SRP enabled exotic orbits. The variations in effective area required for the case presented are small and easily achievable by a variable reflectivity device such as the ones demonstrated on the Ikaros solar sail (Funase, Mori et al. 2010).

Altogether, double-periodic *g'* orbits are perhaps the best candidates for temporary orbiters in the equatorial plane. They provide a good coverage of the sub-solar point and the whole XY plane, without very close approaches to the asteroid surface that could compromise the safety of the spacecraft. For the range of lightness numbers associated to small asteroid spacecraft (20-30), they are stable in the planar motion but present instability in the out-of-plane motion. Furthermore, their orbits are more robust against the introduction of non-sphericity perturbation due to the retrograde motion close to the asteroid (and prograde away from it), assuming again that the asteroid rotational motion is prograde. The associated unstable manifolds can be of use providing access or escape trajectories to and from a hypothetical stand-off point at a safe distance from the asteroid. The eccentricity of the asteroid orbit has not been considered, but similar orbits have been shown to exist. However, if only a few orbits are considered (due to the intrinsic instability and additional perturbations), the effect of the variation of the distance to the Sun in that timeframe is also limited.

6 Conclusions

The Hill problem with solar radiation pressure is a useful dynamical system to study the motion of spacecraft in the vicinity of asteroids orbiting the Sun. This paper has mapped the evolution of the a and g-*g'* families of planar symmetric periodic orbits with the introduction of solar radiation pressure from the original Hill problem to an extreme case with very high lightness number representative of asteroid missions. The structure of the solution space deviates from the original solution map in the original Hill problem, with the g-*g'* family breaking apart into two unconnected families, one of which disappears for high lightness numbers.

Regarding applications for small asteroid exploration, the single periodic branch of the *g'* family has been shown to be unfeasible for realistic asteroid densities and the lightness numbers characteristics of small bodies. For high lightness numbers, eclipses need to be taken into account, as they modify the structure and connections of the families and shape of the orbits, particularly when close to the L_2 point.

The in-plane and out-of-plane stability of the feasible a and *g'* families is also presented. Family a remains unstable as in the traditional Hill problem for all cases, while family *g'* has certain regions of in-plane or out-of-plane stability. However, the most stable branch of this family corresponds to the unfeasible section that intersects the asteroid. The double periodic *g'* branch presents the best characteristics for temporary orbits around a hypothetical small asteroid.

ACKNOWLEDGEMENTS

The work reported was supported by European Research Council grant 227571 (VISIONSPACE). We would also like to acknowledge the John Moyes Lessells Travel Scholarship of the Royal Society of Edinburgh, and the Mac Robertson Postgraduate Travel Scholarship for their support of the PhD placement at CU Boulder that led to the research presented in this paper.

REFERENCES

Batkhin, A. B. (2013a). "Symmetric periodic solutions of the Hill's problem. I." Cosmic Research **51**(4): 275-288.

Batkhin, A. B. (2013b). "Symmetric periodic solutions of the Hill's problem. II." Cosmic Research **51**(6): 452-464.

Broschart, S. B., G. Lantoine, et al. (2013). Characteristics of Quasi-Terminator Orbits Near Primitive Bodies. 23rd Space Flight Mechanics Meeting, Lihue, Kauai, USA.

Broschart, S. B. and D. J. Scheeres (2005). "Control of Hovering Spacecraft Near Small Bodies: Application to Asteroid 25143 Itokawa." Journal of Guidance, Control, and Dynamics **28**(2): 343-354.

Broschart, S. B. and D. J. Scheeres (2007). "Boundedness of Spacecraft Hovering Under Dead-Band Control in Time-Invariant Systems." Journal of Guidance, Control, and Dynamics **30**(2): 601-610.

Broucke, R. (1969). "Stability of Periodic Orbits in the Elliptic, Restricted Three-Body Problem." AIAA Journal **7**(6): 1003-1009.

Broucke, R. A. (1968). Periodic orbits in the restricted three-body problem with Earth-Moon masses. JPL technical report 32-1168. Pasadena, Jet Propulsion Laboratory, California Institute of Technology.

Byram, S. M. and D. J. Scheeres (2008). Spacecraft Dynamics in the Vicinity of a Comet in a Rotating Frame. AIAA/AAS Astrodynamics Specialist Conference, Hololulu, Hawaii, USA.

Chernikov, Y. A. (1970). "The Photogravitational Restricted Three-body Problem." Soviet Astronomy - AJ **13**(1): 176-181.

Chesley, S. R., P. W. Chodas, et al. (2002). "Quantifying the Risk Posed by Potential Earth Impacts." Icarus **159**: 423-432.

Dankowicz, H. (1993). "Some special orbits in the two-body problem with radiation pressure." Celestial Mechanics and Dynamical Astronomy **58**: 353-370.

Darwin, G. H. (1897). "Periodic Orbits." Acta Mathematica **21**(1): 99-242.

Dormand, J. R. and P. J. Prince (1980). "A family of embedded Runge-Kutta formulae." Journal of Computational and Applied Mathematics **6**(1): 19-26.

Farres, A. and A. Jorba (2012). Orbital Dynamics of a Solar Sail near L1 and L2 in the Elliptic Hill Problem. 63rd International Astronautical Congress, Naples, Italy.

Funase, R., O. Mori, et al. (2010). Attitude control of IKAROS solar sail spacecraft and its flight results. 61st International Astronautical Congress 2010, Prague, Czech Republic.

García Yárnoz, D., J. P. Sanchez Cuartielles, et al. (2013). Applications of Solar Radiation Pressure Dominated Highly Non-Keplerian Trajectories around Minor Bodies. 64th International Astronautical Congress, Beijing, China, IAF.

Giancotti, M., S. Campagnola, et al. (2014). "Families of periodic orbits in Hill's problem with solar radiation pressure: application to Hayabusa 2." Celestial Mechanics and Dynamical Astronomy **120**(3): 269-286.

Hénon, M. (1965). "Exploration numérique du problème restreint. II. Masses égales, stabilité des orbites périodiques." Annales d'Astrophysique **28**: 992-1007.

Hénon, M. (1969). "Numerical Exploration of the Restricted Problem. V. Hill's Case: Periodic Orbits and Their Stability." Astronomy and Astrophysics **1**: 223-238.

Hénon, M. (1973a). "Vertical Stability of Periodic Orbits in the Restricted Problem. I. Equal Masses." Astronomy and Astrophysics **28**: 415-426.

Hénon, M. (1973b). "Vertical Stability of Periodic Orbits in the Restricted Problem. II. Hill's Case." Astronomy and Astrophysics **30**: 317-321.

Hénon, M. (2003). "New Families of periodic Orbits in Hill's Problem of Three Bodies." Celestial Mechanics and Dynamical Astronomy **85**(223-246).
Hénon, M. (2005). "Families of Asymmetric Periodic Orbits in Hill's Problem of Three Bodies." Celestial Mechanics and Dynamical Astronomy **93**(1-4): 87-100.
Ichtiaroglou, S. (1980). "Elliptic Hill's Problem: The Continuation of Periodic Orbits." Astronomy and Astrophysics **92**: 139-141.
Ichtiaroglou, S. (1981). "Elliptic Hill Problem: Families of Periodic Orbits." Astronomy and Astrophysics **98**: 401-405.
Kanavos, S. S., V. V. Markellos, et al. (2002). "The Photogravitational Hill Problem: Numerical Exploration." Earth, Moon and Planets **91**: 223-241.
Katherine, Y.-Y. L. and B. Villac (2010). "Periodic orbits families in the Hill's three-body problem with solar radiation pressure." Advances in the astronautical sciences **136**(1): 285-300.
Lara, M. and R. Russell (2006). Concerning the family "g" of the restricted three-body problem. IX Jornadas de Trabajo en Mecanica Celeste, Jaca, Huesca, Spain.
Lara, M., R. Russell, et al. (2007). "Classification of the Distant Stability Regions at Europa." Journal of Guidance, Control, and Dynamics **30**(2): 409-418.
Markellos, V. V., A. E. Roy, et al. (2000). "A Photogravitational Hill Problem and Radiation Effect on Hill Stability of Orbits." Astrophysics and Space Science **271**: 293-301.
Matukuma, T. (1930). "On the Periodic Orbits in Hill's Case." Proceedings of the Imperial Academy of Japan **6**(1): 6-8.
Matukuma, T. (1932). "Periodic Orbits in Hill's Case. Second Paper." Proceedings of the Imperial Academy of Japan **8**(5): 147-150.
Matukuma, T. (1933). "Periodic Orbits in Hill's Case. Third Paper." Proceedings of the Imperial Academy of Japan **9**(8): 364-366.
McInnes, C. R. (1999). Solar Sailing. Technology, Dynamics and Mission Applications. Berlin, Germany, Springer-Verlag, **pp.** 40.
Michalodimitrakis, M. (1980). "Hill's problem: families of three-dimensional periodic orbits." Astrophysics and Space Science **68**(1): 253-268.
Miele, A. (2010). "Revisit of the Theorem of Image Trajectories in the Earth-Moon Space." Journal of Optimization Theory and Applications **147**(3): 483-490.
Nocedal, J. and S. J. Wright (2006). Sequential Quadratic Programming. Numerical Optimization. S. Verlag. New York, Springer Verlag**:** 530-563.
Ocampo, C. A. and G. W. Rosborough (1993). "Transfer trajectories for distant retrograde orbiters of the Earth." Advances in the Astronautical Sciences **82**: 1177-1200.
Papadakis, K. E. (1996). "Families of Periodic Orbits in the Photogravitational Three-Body Problem." Astrophysics and Space Science **245**: 1-13.
Papadakis, K. E. (2006). "The Planar Photogravitational Hill Problem." International Journal of Bifurcation and Chaos **16**(6): 1809-1821.
Perko, L. M. (1982). "Periodic solutions of the restricted problem that are analytic continuations of periodic solutions of Hill's problem for small $\mu>0$." Celestial mechanics **30**(2): 115-132.
Russell, R. P. (2006). "Global search for planar and three-dimensional periodic orbits near Europa." Journal of the Astronautical Sciences **54**(2): 199-226.
Scheeres, D. J. (2007). Orbit Mechanics About Small Asteorids. 20th International Symposium on Space Flight Dynamics, Annapolis, Maryland, USA.
Scheeres, D. J. (2012a). Controlled Hovering Motion at an Asteroid. Orbital Motion in Strongly Perturbed Environments: Applications to Asteroid, Comet and Planetary Satellite Orbiters, Springer-Verlag Berlin Heidelberg**:** 243-254.
Scheeres, D. J. (2012b). Properties of Solution. Orbital Motion in Strongly Perturbed Environments: Applications to Asteroid, Comet and Planetary Satellite Orbiters, Springer-Verlag Berlin Heidelberg**:** 105-141.
Scheeres, D. J. (2012c). Solar Radiation Pressure: Exact Analysis. Orbital Motion in Strongly Perturbed Environments: Applications to Asteroid, Comet and Planetary Satellite Orbiters, Springer-Verlag Berlin Heidelberg**:** 255-275.

Scheeres, D. J. (2012d). Solution and Characterization Methods. Orbital Motion in Strongly Perturbed Environments: Applications to Asteroid, Comet and Planetary Satellite Orbiters, Springer-Verlag Berlin Heidelberg**:** 143-169.

Simmons, J. F. L., A. J. C. McDonald, et al. (1985). "The restricted 3-body problem with radiation pressure." Celestial Mechanics **35**: 145-187.

Simó, C. and T. J. Stuchi (2000). "Central stable/unstable manifolds and the destruction of KAM tori in the planar Hill problem." Physica D: Nonlinear Phenomena **140**: 1-32.

Strömgren, E. (1922). "Forms of periodic motion in the Restricted Problem and in the general Problem of Three Bodies, according to researches executed at the Observatory Copenhagen." Publikationer og mindre Meddeler fra Kobenhavns Observatorium **39**: 3-29.

Szebehely, V. (1967). Theory of orbits. New York, New York, Academic Press, **pp.** 443-555.

Szebehely, V. and P. Nacozy (1967). "A Class of E. Strömgren's Direct Orbits in the Restricted Problem." The Astronomical Journal **72**(2): 184-190.

Takahashi, Y. and D. J. Scheeres (2011). "Small-Body Postrendezvous Characterisation via Slow Hyperbolic Flybys." Journal of Guidance, Control, and Dynamics **34**(6): 1815-1827.

Verrier, P. (2013). Connections between Halo families and prograde families in the Earth-Moon CRTBP. (unpublished), University of Strathclyde**:** 1-11.

Villac, B. F. (2003). Dynamics in the Hill problem with applications to spacecraft maneuvers. Aerospace Engineering. Ann Arbor, The University of Michigan.

Voyatzis, G., I. Gkolias, et al. (2012). "The dynamics of the elliptic Hill problem: periodic orbits and stability regions." Celestial Mechanics and Dynamical Astronomy **113**(1): 125-139.

APPENDIX A The L_1 point region and additional families c and f

The main body of this paper deals with Hill problem a and g-*g'* planar families of orbits. These families either originate from the L_2 point or are constraint in their excursions away from the asteroid by the zero velocity curves at energies similar to that of L_2. This feature can be practical for minor body observations, as the L_2 point is drawn towards the secondary with increasing solar radiation pressure (see Figure A-1 left), and the associated region of the phase space shrinks, allowing close observations.

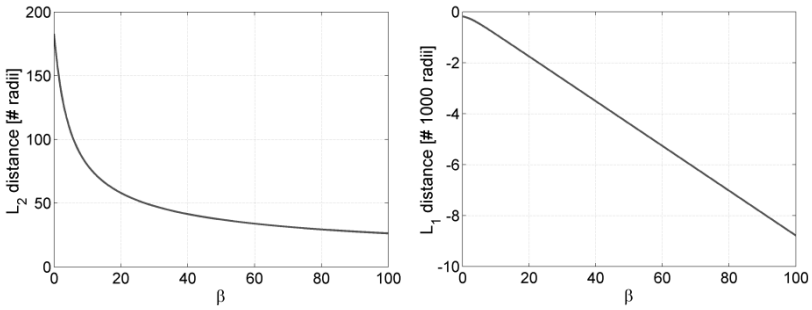

Figure A-1: L_2 and L_1 position with lightness number, assuming an asteroid density of 2.6 g/cm^3.

The L_1 point on the other hand is displaced sunward as the lightness number β increases and quickly escapes the close vicinity of the secondary, as shown in Figure A-1 right. For example, for a lightness number of 30, representative of current and planned missions to asteroids, the L_2 point would be situated at a distance of about 48 radii of the secondary (compared to 183 radii for the case of no SRP), while the L_1 distance is over 2600 radii away from the secondary. In the extreme case of $\beta \sim 684$, the L_2 point stands at merely 10 asteroid radii, while L_1 is over 60000 radii away. Note that the vertical scale of the L_1 plot is given in thousands of radii. The region of the phase space around L_1, together with families originating from it or constraint to this region, is expected to display much larger distances to the secondary. This was already advanced by Farres and Jorba (2012) when they studied the use of a solar sail around asteroid Vesta.

To illustrate this fact, the phase space for negative ξ_0 crossings has been mapped in Figure A-2 for a particular relatively small lightness number of $\beta = 10$, which is still below most minor body missions SRP levels. It is important to note the complete loss of symmetry in the positions and energies of the two libration points, and the associated forbidden regions. The upper right corner of Figure A-2 corresponds to the $\beta = 10$ plot of Figure 4.

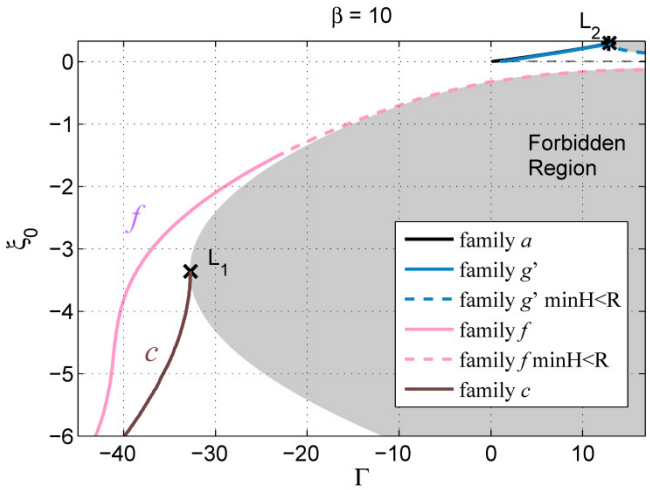

Figure A-2: Solution map including L_1 vicinity for lightness number $\beta = 10$.

When comparing this map to the original Hill problem map in Figure 2, it is possible to observe that both families c and f are drawn towards the border of the forbidden region, which consists of degenerate 'linear' orbits along the horizontal axis. This is particularly noticeable for the region of family f with closer ξ_0 crossings, resulting in orbits that intersect the body of the secondary. Sections of the orbit families that have a minimum distance to the secondary of less than one radius have been indicated in Figure A-2 with a discontinuous line, assuming an asteroid density of 2.6 g/cm^3.

Figure A-3 plots a few example members of families c (left) and f (right) for this particular SRP level. The planar Lyapunov orbits of the c family have an almost elliptical shape centred on L_1, with only orbits at very low Jacobi constant starting to display the bean-shape deformations typical of the planar Lyapunov family. This was observed to a lesser extent by Katherine and Villac (2010) for a lower lightness number $\beta = 2.515$. Orbits of the f family (plotted on Figure A-3 right) have lost their typical quasi-elliptical shape in the traditional Hill case and have a more tear-like shape, with a very close approach to the secondary over the antisolar point. Figure A-4 left shows a detail of this close approach, where the asteroid or secondary surface is represented with dashed concentric circles for three different densities (1, 2 and 3 g/cm^3). As evidenced in Figure A-4 right, family f orbits with ξ_0 crossings lower than 390 secondary radii all intersect the secondary (dashed line). For this SRP level this is about half the distance to the L_1 point. It can be observed that the close approach still takes place for orbits at much larger distances (close approaches as low as 35 secondary radii for orbits of sizes about twice the L_1 distance).

For higher levels of SRP characteristic of asteroids and comets, the distances to L_1 would increase, the size and periods of the c and f orbits would also grow, and larger portions of the f family would intersect the secondary. All these facts work against the feasibility of realistically using these orbits for close minor body observations, in spite of their attractiveness.

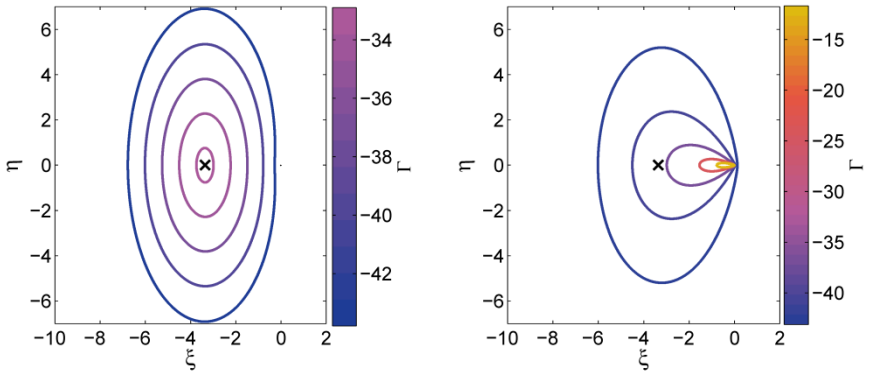

Figure A-3: Families c (left) and f (right) for a lightness number $\beta = 10$. The x marker indicates the L_1 point position.

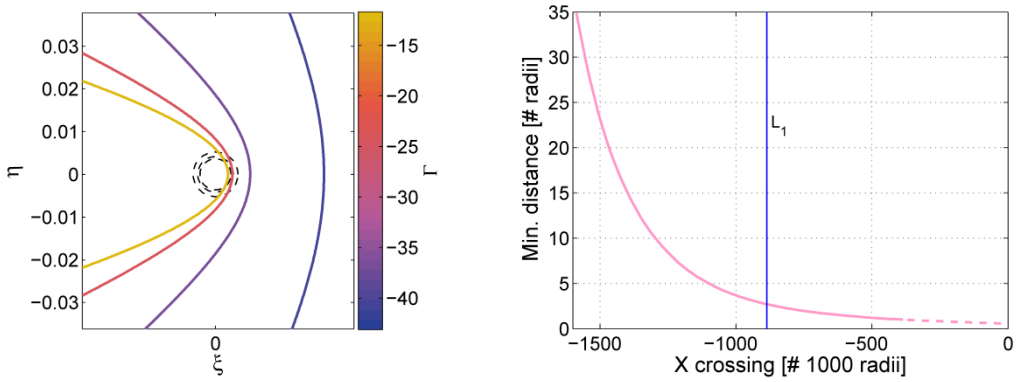

Figure A-4: Detail on family f for a lightness number $\beta = 10$. Orbits with high Jacobi constant intersect the asteroid.